$LaSi_3N_5$, which has had its crystal structure determined,[27] such SiN_4 tetrahedra are present. This is the first observation of nonbridging SiN_4 tetrahedra by solid-state NMR.

The shift ranges summarized in Figure 8 show a general trend to more positive chemical shifts with increasing nitrogen coordination of silicon, consistent with the changing covalency of the bonds. As the Si–N bond is more covalent than the Si–O bond, the replacement of oxygen by nitrogen increases the average bond covalency, leading to a deshielding of the silicon, making the chemical shift of each successive $SiO_{4-x}N_x$ (increasing x) more positive. However, from the shifts presented here it can be seen that there is no strict ordering of the shifts, with the SiO_2N_2-$Q^{(2)}$ in $YSiO_2N$ at a more negative chemical shift than SiO_2N_2-$Q^{(3)}Q^{(4)}$ in $Y_2Si_3O_3N_4$. However, as for previous studies on silicates, there can be expected to be an extensive overlap of the shift ranges of the different structural units, reflecting the fact that the NMR chemical shift is an involved function of the structure. In other, mainly solution-state studies of SiX_aY_b $(a + b = 4)$ tetrahedra, the chemical shift rarely follows a linear variation with some intermediate member having the largest p-electron imbalance about the silicon and thus having the most paramagnetic shift.[28] It is quite likely therefore that the chemical shift difference between successive SiO_xN_{4-x} tetrahedra is nonlinear (and possibly not monotonic), enhancing the overlap of the chemical shift ranges.

Conclusion

The chemical shifts for all tetrahedra SiO_xN_{4-x} $(0 \le x \le 4)$ can now be given from the MAS NMR spectra of the Y–Si–O–N crystalline phases. The general trend to more positive chemical shifts with increasing nitrogen may be attributed to the greater covalency of the bonds. The extensive overlap of the chemical shifts of different tetrahedral units means that no resonance can be unambiguously assigned to a given unit (as with silicates) if no other information is available. MAS NMR can be used in exactly the same manner as XRD to identify phases once a catalog of chemical shifts has been established. This has been demonstrated for *N*-apatite and *N*-melilite with the additional advantage that the spectra can be made truly quantitative. The sensitivity of the chemical shift to the local environment is a useful aid to structural studies of these phases. This has allowed us to refine the structures of *N*-YAM and *N*-melilite. To obtain a better understanding of the influences on the ^{29}Si chemical shift in the solid state the range of compounds studied containing SiO_xN_{4-x} tetrahedra will have to be further expanded.

Acknowledgment. We thank the SERC for support and a studentship (M.E.S.).

Registry No. Y, 7440-65-5; Si, 7440-21-3; O_2, 7782-44-7; N_2, 7727-37-9; $Y_2Si_3O_3N_4$, 54650-98-5; $Y_2Si_2O_7$, 14286-95-4; Y_2SiO_5, 12027-88-2; $Y_4Si_2O_7N_2$, 58694-26-1; $YSiO_2N$, 62361-78-8; Si_3N_4, 12033-89-5; Si_2N_2O, 12033-76-0; $Y_5Si_3O_{12}N$, 59977-54-7; YSi_3N_5, 112068-60-7.

---

[27] Inoue, Z.; Mamoru, M. *J. Mater. Sci.* **1980**, *15*, 2915–2920.
[28] Tossell, J. A.; Lazzeretti, P. *Chem. Phys. Lett.* **1986**, *133*, 463–465.

Equilibrium Isotope Effects on the Hydration of Gas-Phase Ions. The Effect of Hydrogen Bond Formation on Deuterium Isotopic Fractionation Factors for H_3O^+, $H_5O_2^+$, $F(H_2O)^-$, and $Cl(H_2O)^-$

J. W. Larson and T. B. McMahon*

Contribution from the Department of Chemistry and Guelph-Waterloo Centre for Graduate Work in Chemistry, University of Waterloo, Waterloo, Ontario, Canada N2L 3G1.
Received May 4, 1987

Abstract: Equilibrium isotope exchange reactions have been examined for transfer of $H^+(D^+)$, $H_3O^+(H_2OD^+$, HOD_2^+, $D_3O^+)$, F^-, and Cl^- among H_2O, HOD, and D_2O. In each case ions are found to be more favorably coordinated to H_2O rather than D_2O. These results are compared to similar data for ions in H_2O or D_2O solution. Statistical thermodynamic arguments are presented which imply that rotational effects play an important role in determination of the overall isotope effect, in addition to the more commonly considered zero-point energy effects. The important role of the inversion mode of H_3O^+ on the isotope effect is considered. Implications for isotope fractionation in the interstellar medium are discussed.

The examination of solvent isotope effects has been used extensively as a probe of the nature of hydrogen-bonded interactions between solute and solvent species.[1] In some situations the general observation has been made that interactions of strong acids with solvent favor deuterium bonds, while weak acids interact preferentially via hydrogen bonds.[2] This statement, while appearing to be borne out by limited experimental data, has not been explained fully on a rational physical basis.

It has been shown recently from studies of gas-phase hydronium ion in this laboratory[3] that the claim that in general hydrogen will accumulate in species where the site of isotopic substitution is in the lower force field appears to be true. This result was attributed to be a direct consequence of a greater zero-point energy difference between H_3O^+ and D_3O^+ relative to that between H_2O and D_2O. However, in another study of isotopic fractionation in the $ClHCl^-$–$ClDCl^-$ system[4] it was shown that, particularly for small ions, differences in rotational partition functions due to significant differences in moments of inertia can dominate the isotope effect. This effect was shown to reinforce that of the vibrational zero-point

---

[1] (a) Kreevoy, M. M. In *Isotope Effects in Organic Chemistry*; Buncel, E., Lee, C. C., Eds.; Elsevier: Amsterdam. 1976; Vol. 2. (b) More O'Ferrall, R. A. In *Proton Transfer Reactions*; Caldin, E. C., Gold, V., Eds.; Chapman and Hall: London, 1975. (c) Schowen, R. L. *Prog. Phys. Org. Chem.* **1972**, *9*, 275. (d) Schowen, R. L. In *Isotope Effects on Enzyme Catalyzed Reactions*; Cleland. W. N., O'Leary, M. H., Northrup, D. B., Eds.; University Parke Press: Baltimore, MD, 1977. (e) Lias, S. G. *J. Phys. Chem.* **1984**, *88*, 4401.

[2] Joesten, M. D.; Schaad, L. J. *Hydrogen Bonding*; Marcel-Dekker: New York, 1974.

[3] Larson, J. W.; McMahon, T. B. *J. Am. Chem. Soc.* **1986**, *108*, 1719.

energy differences in the bichloride case leading to favoring of hydrogen versus deuterium bonds.

These two investigations[3,4] have been the only attempt to date to experimentally probe the nature of equilibrium isotope effects in solvated gaseous ions. Other recent work from this laboratory has resulted in demonstration of methods for the bimolecular generation of solvated cations[5] and anions[6-8] under the low-pressure conditions of pulsed ion cyclotron resonance experiments. In the present manuscript we have exploited these techniques for the purpose of examination of hydrated H_3O^+, F^-, and Cl^-. Each of these species participates in a strong hydrogen-bonded interaction with H_2O of 32, 23, and 14 kcal mol^{-1}, respectively. These species provide an important link between naked ions typically studied in the gas phase and fully solvated ions studied in solution. The deuterium isotope effect for the single hydration of these ions can potentially provide valuable clues to the nature of the hydrogen-bonded interaction. In addition the species under investigation also serve as useful models for intermediates or transition states in proton-transfer reactions and acid catalysis and may potentially provide insight into the kinetics of these processes.[9]

The equilibrium results presented here also provide some prediction of possible deuterium fractionation in the interstellar medium. If the major chemical processes in interstellar clouds are in fact ion-molecule reactions, then these data can be used to explain isotopic abundances of ions other than the naturally occurring abundance of neutrals.

Experimental Section

All experiments were carried out at *ambient temperature* (25 °C) with an ion cyclotron resonance spectrometer of basic Varian V-5900 design which has been extensively modified to permit routine operation in both conventional drift and pulsed modes. Multiple exchange reactions and nonreactive collisions ensure that ions are at thermal equilibrium with the neutral gas. Details of the design and operation of pulsed ion cyclotron resonance and both conventional single and double resonance experiments have been described in detail elsewhere.[10,11]

A mixture of H_2O and D_2O (Merck, Sharpe and Dohme of Canada, Ltd. 99.5 + atom%) was made up by weight and transferred to a glass vessel of roughly 500-mL capacity. One mixture contained approximately 1 g of each component, while the second contained 10 g of each. These quantities are sufficiently large that the amount used in all subsequent experiments was small enough to maintain a constant composition in the liquid phase throughout.

Samples of H_2O/D_2O admitted to the ICR spectrometer were allowed to equilibrate with the walls of the vacuum inlet system for 1 h following which a single resonance mass spectrum at low pressure was taken to determine the H_2O/D_2O ratio. Following this the inlet system was evacuated, a fresh portion of the H_2O–D_2O mixture was admitted and allowed to equilibrate 1 h, and a mass spectrum was again taken. After the first three additions the H_2O/D_2O ratio was found to remain constant. This procedure was absolutely essential to ensure that no change in the H_2O–D_2O ratio occurred during the course of the isotope effect experiments.

The single resonance mass spectra of H_2O–D_2O mixtures at 10^{-7} Torr showed prominent peaks at *m/z* 18, 19, and 20 corresponding primarily to H_2O^+, HOD^+, and D_2O^+. Much smaller peaks at *m/z* 17 (OH^+) and *m/z* 21 $HOD_2{}^+$ were also present. The *m/z* 17 peak was used to correct the *m/z* 18 intensity for OD^+ assuming statistical fragmentation of the H_2O, HOD, and D_2O neutrals present. The *m/z* 21 peak was used to correct the *m/z* 19 intensity for H_3O^+ and the *m/z* 20 intensity for H_2OD^+, again assuming a statistical isotope distribution. These corrections were in all cases less than 2%. For example in the case of the second mixture the mole fractions of H_2O, HOD, and D_2O obtained were 0.28, 0.48, and 0.24, respectively. These may be compared with the values of 0.263, 0.504, and 0.233 calculated from the known weight composition of the mixture and the liquid–vapor equilibrium data for H_2O, HOD, and D_2O of Narten.[12] We have assumed that these calculated values are very likely more accurate than those obtained from our mass spectrometric analysis, and these have been used in all subsequent calculations. In any case the difference is extremely small and affects the equilibrium data very little.

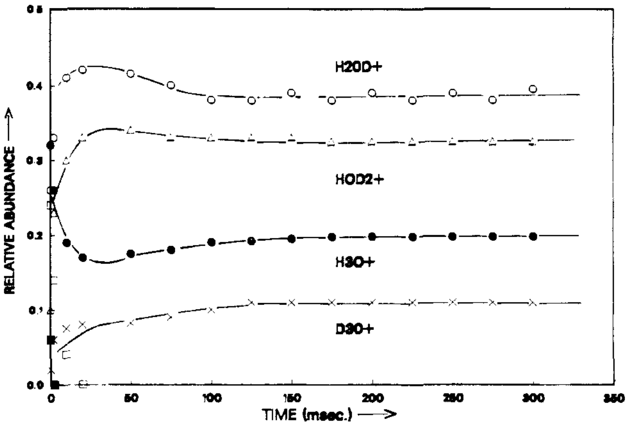

Figure 1. Variation of relative abundances of isotopic hydronium ions with time in a 0.265:0.494:0.241 mixture of $H_2O/HOD/D_2O$ at a total pressure of 1×10^{-6} Torr following a 5-ms, 70-eV electron beam pulse.

Table I. Ion Fractions in Equilibrium with Water Vapor with Mole Fractions of H_2O, DOH, and D_2O of 0.265, 0.494, and 0.241[a]

ion	ion fraction[b]	*n*	K_2	ϕ[c]
H_3O^+	0.198			
		0	2.07	0.64
D_2HO^+	0.387			
		1	0.85	0.79
D_2HO^+	0.314			
		2	0.35	0.97
D_3O^+	0.109			

[a] Calculated from $X_{H_2O}(l) = 0.495$ and ref 14. [b] Total uncertainties in ion fractions are about 0.025 based on double the standard deviation within any single determination or on comparison of the results from the two separate mixtures. [c] Fractionation factor with respect to *liquid* D_2O and H_2O. Uncertainties are about ±0.10.

The reproducibility of the experiments was established by running the same and new mixtures more than 10 months apart to yield virtually identical results.

The reagents used for generation of hydrated ions ($(CHF_2)_2O$, NF_3, $ClCO_2C_2H_5$, and HCO_2CH_3) were all obtained from commercial sources and were used without further purification with the exception of successive freeze–pump–thaw cycles.

Results and Discussion

1. Hydronium Ion, L_3O^+ (L = H, D). Reaction of molecular ions L_2O^+ with L_2O rapidly produces hydronium ions L_3O^+, eq 1.

$$L_2O^+ + L_2O \rightarrow L_3O^+ + OL \qquad (1)$$

A typical plot of ion intensity as a function of trapping time at a total L_2O pressure of 1×10^{-6} Torr is shown in Figure 1. All L_2O^+ species have completely reacted away by 25 ms under these conditions, and a steady-state distribution of the various L_3O^+ species is established by 100 ms. Ion ejection experiments readily established that in H_2O, HOD, and D_2O mixtures all of the L_3O^+ species are reactively coupled by proton- and deuteron-transfer reactions confirming that the steady-state intensities are the result of dynamic equilibrium of L_3O^+ with L_2O vapor. Equilibrium ion and neutral fractions are given in Table I together with the equilibrium constants for the three possible variations of eq 2. In

$$H_{3-n}D_nO^+(g) + \frac{1}{2}D_2O(g) \rightleftarrows H_{2-n}D_{n+1}O^+(g) + \frac{1}{2}H_2O(g) \qquad (2)$$

---

(4) Larson, J. W.; McMahon, T. B. *J. Phys. Chem.* **1987**, *91*, 554.
(5) Larson, J. W.; McMahon, T. B. *J. Am. Chem. Soc.* **1982**, *104*, 6255.
(6) Larson, J. W.; McMahon, T. B. *J. Am. Chem. Soc.* **1983**, *105*, 2944.
(7) Larson, J. W.; McMahon, T. B. *J. Am. Chem. Soc.* **1984**, *106*, 517.
(8) Larson, J. W.; McMahon, T. B. *J. Am. Chem. Soc.* **1987**, *109*, 6230.
(9) Laughton, P. M.; Robertson, R. E. In *Solute–Solvent Interactions*; Coatzee, J. F., Ritchie, C. D., Eds.; Marcel-Dekker; New York, 1969.
(10) McMahon, T. B.; Beauchamp, J. L. *Rev. Sci. Instrum.* **1973**, *43*, 509.
(11) Lehman, T. A.; Bursey, M. M. *Ion Cyclotron Resonance Spectroscopy*; Wiley-Interscience: New York, 1976.
(12) (a) Narten, A. *J. Chem. Phys.* **1964**, *41*, 1318. (b) Narten, A. *J. Chem. Phys.* **1965**, *42*, 814. (c) Friedman, L.; Shiner, V. *J. Chem. Phys.* **1966**, *44*, 4639. (d) Pryer, J. W.; Newbury, R. S.; Barton, G. W. *J. Chem. Phys.* **1967**, *46*, 2253.

solution phase work similar equilibria are frequently expressed as fractionation factors, ϕ, that give, on a per hydrogen basis with statistical effects removed, the change in the environment of the hydrogen atom relative to that in *liquid* water.[1a,d] The individual values of fractionation factors for the sequential replacement of hydrogen by deuterium in hydronium ion are also reported in Table I. These values are obtained by multiplying the equilibrium constants, K_2 by 0.93, the fractionation factor for gaseous water, eq 3, and dividing by the statistical factors of 3, 1, and $^1/_3$,

$$\frac{1}{2}H_2O(g) + \frac{1}{2}(D_2O)(l) \rightleftharpoons \frac{1}{2}D_2O(g) + \frac{1}{2}H_2O(l) \qquad (3)$$

respectively. In most solution phase examinations of hydronium ion it has been customary to assume that each successive replacement of hydrogen by deuterium in L_3O^+ has the same fractionation factor. However, the present results reveal an apparent trend of increasing fractionation factor with increasing deuterium content. The differences in fractionation factor are significantly greater than experimental uncertainties and thus represent real differences. The consequences of this difference for solution phase data are minimal, affecting H_2O/D_2O solvent systems only to a minor extent.

Experiments on solution phase isotope effects usually involve a comparison of results in pure D_2O relative to those in pure H_2O.[13,14] For such experiments the equilibrium constant and fractionation factor for eq 4 are of particular interest. The

$$2H_2O^+(g) + 3D_2O(l) \rightarrow 2D_3O^+(g) + 3H_2O(l) \qquad (4)$$

gas-phase value of K_4 of 0.25 ± 0.03 for hydronium ion can be compared to the aqueous value for the same ion of 0.11.[15] Similarly the gas-phase fractionation factor of L_3O^+ is 0.79 ± 0.01 compared to the solution phase value of 0.69 ± 0.02. It is of interest to note that the gas-phase value is virtually identical with that obtained for the hydronium ion in acetonitrile solution.[16] It has been abundantly demonstrated that hydrogen bonding lowers fractionation factors.[17] Thus the decrease in fractionation factor in proceeding from unsolvated hydronium ion to the fully hydrated aqueous ion may be ascribed to the extensive hydrogen-bonding network in solution. It is noteworthy however that this difference is much less than the difference between the fractionation factor for gaseous water and that for gaseous hydronium ion. It might therefore be tempting to conclude that the presence of the positive charge results in a lowering of the force field of the hydrogens asnd is more important in affecting the fractionation factor than the hydrogen bonding.

2. Hydrated Hydronium Ion, $L_5O_2^+$. Production of the singly hydrated hydronium ion was accomplished under low-pressure ICR conditions by fast bimolecular ion-molecule reactions occurring in mixtures containing $\alpha,\alpha,\alpha',\alpha'$-tetrafluorodimethyl ether, $(CHF_2)_2O$.[5,8] These sequences involving H_2O are outlined in eq 5–8. At pressures of L_2O and $(CFF_2)_2O$ at a total of 3×10^{-6}

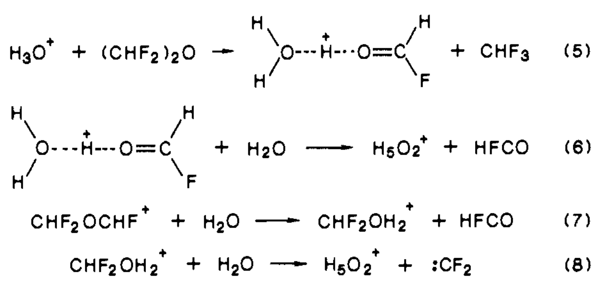

Torr steady-state distributions were obtained by 150 ms, and

Table II. Ion Fractions in Equilibrium with Water Vapor with Mole Fraction Neutrals as in Table I

ion	ion fraction[a]	n	K_9 exptl	K_9 calcd
$H_5O_2^+$	0.074			
		0	3.37	4.13
$H_4DO_2^+$	0.238			
		1	1.49	1.62
$H_3D_2O_2^+$	0.339			
		2	0.75	0.87
$H_2D_3O_2^+$	0.242			
		3	0.39	0.35
HD_4O_{2+}	0.091			
		4	0.18	0.15
$D_5O_2^+$	0.016			

[a] Uncertainties are approximately ±0.007.

intensities were then monitored for a further 500 ms. Equilibrium ion distributions for the H_2O, HOD, and D_2O mixtures used above are reported in Table II together with the calculated equilibrium constants for eq 9 where $n = 0$–4. An average fractionation factor for gaseous $L_5O_2^+$ may be calculated from the equilibrium constant for eq 10. The value of ϕ_9, given by eq 11, of 0.73 ± 0.05 is

$$H_{5-n}D_nO_2^+(g) + \frac{1}{2}D_2O(g) \rightleftharpoons H_{4-n}D_{n+1}O_2^+(g) + \frac{1}{2}H_2O(g) \qquad (9)$$

$$2H_5O_2^+(g) + 5D_2O(l) \rightleftharpoons 2D_5O_2^+(g) + 5H_2O(l) \qquad (10)$$

$$\phi_9 = K_9^{1/10} \cdot K_3 \qquad (11)$$

intermediate between that for gaseous L_3O^+ (0.79) given above and that for aqueous L_3O^+ (0.69). This result is qualitatively reasonable since the average environment of hydrogen atoms in $H_5O_2^+$ is intermediate between that of gaseous H_3O^+ and extensively hydrated H_3O^+.

In $L_5O_2^+$ there are two very different hydrogen environments, the terminal hydrogens more closely resembling free H_3O^+ and the bridging hydrogen more closely resembling the average environment of a hydrogen-bond position for the proton in aqueous solution. Each of these different positions will have a different fractionation factor ϕ_t and ϕ_b and will contribute to ϕ_9 as given in eq 12. In the absence of any further data ϕ_b and ϕ_t are not

$$\phi_9^5 = \phi_t^4 \phi_b \qquad (12)$$

separable from experimental data for ϕ_9. However, an approximate solution may be obtained by estimating ϕ_t to be the geometric mean of fractionation factors for gaseous L_2O and L_3O^+. The value for ϕ_t of 0.86 thus obtained allows estimation of ϕ_b as 0.38. Low values of fractionation factor such as this have previously been shown to be associated with protons residing in broad flat minima similar to that determined by ab initio calculation to be the case for $H_5O_2.^+$.[19] In order to obtain some measure of the validity of this separation of fractionation factors equilibrium constants K_9 have been calculated from these values of ϕ_b and ϕ_t by calculation of the fraction of each of the 12 microscopically distinct $L_5O_2^+$ species present. These values are also reported in Table II. The agreement between experimental and calculated values of K_9, while fair, is hampered by the assumptions made that ϕ_b is not affected by whether the terminal positions are hydrogen or deuterium and that ϕ_t is not affected by whether the bridging position is hydrogen or deuterium.

3. Hydrated Fluoride Ion. The production of hydrated fluoride by bimolecular ion-molecule reaction has previously been demonstrated in this laboratory by the reaction of the ion derived from deprotonation of 2-fluoropropene with water.[6,20] It has also been demonstrated that the fluoride donor involved is very likely a

---

[13] Salomaa, P.; Aalto, V. *Acta Chem. Scand.* **1966**, *20*, 2035.

[14] Salomaa, P. *Acta Chem. Scand.* **1971**, *25*, 24.

[15] Bell, R. F. *The Proton in Chemistry*, 2nd ed.; Chapman-Hall: 1973.

[16] Kurz, J. L.; Myers, M. T.; Ratcliffe, K. M. *J. Am. Chem. Soc.* **1984**, *106*, 5631.

[17] Kreevoy, M. M.; Liang, T.-M.; Chang, K. C. *J. Am. Chem. Soc.* **1977**, *99*, 5207.

[18] Clair, R. L.; McMahon, T. B. *Can. J. Chem.* **1980**, *58*, 863.

[19] Del Bene, J. E.; Frisch, J. J.; Pople, J. A. *J. Phys. Chem.* **1985**, *89*, 3669.

[20] McMahon, T. B.; Northcott, C. J. *Can. J. Chem.* **1978**, *56*, 1069.

Table III. Ion Fractions of $(L_2O)F^-$ in Equilibrium with Water Vapor with Mole Fractions[a] of H_2O, HOD, and D_2O Equal to 0.263, 0.493, and 0.243, Respectively

ion	ion fraction[b]	n	$K_{16,17}$
$(H_2O)F^-$	0.36		
		0	1.21
$(DHO)F^-$	0.42		
		1	0.54
$(D_2O)F^-$	0.22		

[a] Calculated from $X_{H_2O}(l) = 0.493$. [b] Small corrections to $I(HOHF^-)$ were made for $I(^{37}Cl^-)$.

hydrogen-bonded fluoride–allene complex rather than a 2-fluoroallyl anion.[21] The relevant reaction sequence is outlined in eq 13–15. In mixtures of H_2O, HOD, and D_2O fluoride

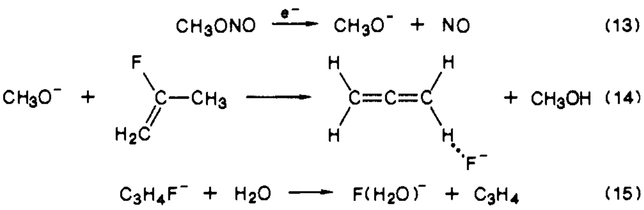

exchange occurs rapidly leading to the equilibrium anonic abundances given in table III. Equilibrium constants for the exchange reactions, eq 16–17 are also given in Table III.

$$(H_2O)F^- + HOD \rightleftarrows (HOD)F^- + H_2O \quad (16)$$

$$(HOD)F^- + D_2O \rightleftarrows (D_2O)F^- + HOD \quad (17)$$

The fractionation factors for the binding of F^- to L_2O are given by the product of K_3 and the equilibrium constants for eq 18 and 19.

$$(H_2O)F^-(g) + \frac{1}{2}D_2O(g) \rightleftarrows (HOD)F^-(g) + \frac{1}{2}H_2O(g) \quad (18)$$

$$(HOD)F^-(g) + \frac{1}{2}(D_2O)(g) \rightleftarrows (D_2O)F^-(g) + \frac{1}{2}H_2O(g) \quad (19)$$

$$0.93K_{18} = \phi_{18} = 1.13 \quad (20)$$

$$0.93K_{19} = \phi_{19} = 0.51 \quad (21)$$

If the fractionation factors for the terminal and bridging hydrogens in $(L_2O)F^-$ are independent of each other, then the values ϕ_t and ϕ_b, respectively, can be calculated from ϕ_{17} and ϕ_{18} by eq 22 and 23. No real solutions exist to this pair of equations,

$$\phi_{18} = \phi_t + \phi_b \quad (22)$$

$$\phi_{19} = \frac{\phi_t\phi_b}{\phi_t+\phi_b} \quad (23)$$

however, indicating that ϕ_b and ϕ_t are in fact coupled. This fact may also be illustrated by examination of eq 24. Again considering ϕ_b and ϕ_t to be independent of each other eq 25 is obtained for K_{24}. The minimum value obtainable for K_{24} under these circumstances is 4.0 when $\phi_b = \phi_t$ since all other values of ϕ_b and ϕ_t lead to larger values of K_{24}. The experimentally determined value of K_{24} is 2.2 ± 0.4 again indicating that ϕ_b and ϕ_t are directly coupled. The net effect of the coupling of ϕ_b and ϕ_t is such that the $(HOD)F^-$ isotopomer is less stable than would be predicted from the equilibrium abundances of $(H_2O)F^-$ and $(D_2O)F^-$ and the rule of the geometric mean. Similar, but smaller, effects have been previously noted in neutral water, the hydronium ion, and hydrated hydronium ion.

$$(H_2O)F^- + (D_2O)F^- \rightleftarrows 2(HOD)F^- \quad (24)$$

$$K_{24} = \left[\frac{(\phi_b + \phi_t)^2}{\phi_b\phi_t}\right] \quad (25)$$

Table IV. Ion Fractions of $(L_2O)Cl^-$ in Equilibrium with Water Vapor of the Composition Given in Table III

ion	ion fraction[a]	n	$K_{31,32}$
$(H_2O)Cl^-$	0.34		
		0	1.25
$(DHO)Cl^-$	0.41		
		1	0.61
$(D_2O)Cl^-$	0.24		

[a] $I(H_2OCl) = {}^4/_3I_{53}$; $I(DHOCl) = I_{54} + I_{56}$; $I(D_2OCl) = I_{55} - {}^1/_3(I_{53} + I_{57})$·±0.015.

4. Hydrated Chloride Ion. Production of chloride ion adducts has previously been demonstrated to be efficiently and generally accomplished by chloride transfer from chloroformate ion generated by negative ion molecule reaction sequences in ethyl chloroformate,[7,22] eq 26–28. In the presence of H_2O, HOD, and D_2O mixtures chloride exchange equilibrium among the various isotopic water molecules is readily established, eq 29–30.

$$e^- + ClCO_2C_2H_5 \rightarrow Cl^- + CO_2C_2H_5 \quad (26)$$

$$Cl^- + ClCO_2C_2H_5 \rightarrow ClCO_2^- + C_2H_5Cl \quad (27)$$

$$ClCO_2^- + H_2O \rightarrow Cl(H_2O)^- + CO_2 \quad (28)$$

$$Cl^-(H_2O) + HOD \rightleftarrows Cl^-(HOD) + H_2O \quad (29)$$

$$Cl^-(HOD) + D_2O \rightleftarrows Cl^-(D_2O) + HOD \quad (30)$$

Equilibrium ion abundances for a typical H_2O, HOD, and D_2O mixture are given in Table IV together with the equilibrium constants for eq 31 and 32. The fractionation factors for eq 31 and 32 are given, in the same manner as described above for hydrated fluoride ion, by eq 33 and 34. The values of the equilibrium constants for the individual reactions are slightly greater for chloride ion than for the analogous fluoride reactions. In addition the average fractionation factor for chloride of 0.87 is closer to the value for free water, a consequence of the weaker interaction of Cl^- with L_2O relative to F^- and hence a smaller perturbation of the force field of the hydrogens of the water molecule. As for the fluoride case the values of these fractionation factors indicate that the values of ϕ_b and ϕ_t are coupled.

$$Cl^-(H_2O) + \frac{1}{2}D_2O(g) \rightleftarrows Cl^-(HOD) + \frac{1}{2}H_2O \quad (31)$$

$$Cl^-(HOD) + \frac{1}{2}D_2O(g) \rightleftarrows Cl^-(D_2O) + \frac{1}{2}H_2O \quad (32)$$

$$0.93K_{31} = \phi_{31} = 1.17 \quad (33)$$

$$0.93K_{32} = \phi_{32} = 0.57 \quad (34)$$

5. Statistical Thermodynamic Calculations. The magnitude of each of the isotope effects experimentally determined here can, in principle, be calculated from standard statistical thermodynamic relationships. For the general equilibrium, eq 35, the equilibrium constant is given by eq 36 where the Q's are the total partition functions of each species and Δzpe is the zero-point energy change in proceeding from reactants to products. Each partition function can be expressed as a product of contributions from translational, rotational, and vibrational motions. The translational component is straightforwardly calculated from the known masses of reactants and products. The rotational component may also be calculated from moments of inertia for each species which are obtainable from the experimental geometries of H_2O and D_2O and from ab initio calculations for each of the ions involved. The geometries of each of these ionic species have been obtained from large basis set ab initio calculations, and the geometries are expected to be

$$A^{\pm}(H_2O)n(g) + nD_2O(g) \rightleftarrows A^{+}(D_2O)n(g) + nH_2O(g) \quad (35)$$

$$K_{eq} = \frac{Q_{A\pm}(H_2O)_n{\cdot}Q^nH_2O}{Q_{A\pm}(H_2O)_n{\cdot}Q^nD_2O}\cdot e^{-\Delta zpe/RT} \quad (36)$$

---

(21) Roy, M.; McMahon, T. B. *Can. J. Chem.* **1985**, *63*, 708.

(22) Larson, J. W.; McMahon, T. B. *Can. J. Chem.* **1984**, *62*, 675.

Table V. Comparison of Partial Statistical Thermodynamic and Experimental Equilibrium Constants for Selected Isotropic Replacement Reactions

reaction	K_{trans}	K_{rot}	K_{MMI}	K_{exptl}
1. $H_3O^+ + {}^3/_2D_2O \rightleftarrows D_3O^+ + {}^3/_2H_2O$	0.99	0.65	0.64	0.62
2. $H_3O^+ + {}^1/_2D_2O \rightleftarrows H_2OD^+ + {}^1/_2H_2O$	1.0	2.70	2.70	2.1
3. $H_2OD^+ + {}^1/_2D_2O \rightleftarrows HOD_2^+ + {}^1/_2H_2O$	0.99	0.87	0.86	0.85
4. $HOD_2^+ + {}^1/_2D_2O \rightleftarrows D_3O^+ + {}^1/_2H_2O$	0.99	0.28	0.27	0.35
5. $H_5O_2 + {}^5/_2D_2O \rightleftarrows D_5O_2^+ + {}^5/_2H_2O$	0.81	0.16	0.13	0.27
6. $F(H_2O)^- + D_2O \rightleftarrows F(D_2O)^- + H_2O$	0.92	0.54	0.50	0.66
7. $Cl(H_2O)^- + D_2O \rightleftarrows Cl(D_2O)^- + H_2O$	0.90	0.56	0.50	0.76

very accurate.[23,24,28] The geometries of neutrals and ions as well as the calculated moments of inertia are summarized in Table VI. The vibrational contribution to the overall equilibrium constant cannot be rigorously assessed, however, since the vibrational frequencies of the ionic species are not experimentally known with the exception of the υ_2 and υ_3 modes of H_3O^+[27,28] and the υ_2 mode of D_3O^+.

Even though it is not possible to completely recalculate the equilibrium constant for the various isotope replacement reactions, it is nevertheless instructive to compare the values calculated from translational and rotational components to the experimentally determined quantities. Following the treatment by Melander and Saunders[27] the overall equilibrium constant is divided into components labeled MMI to account for the ratios of masses and moments of inertia arising from the translational and rotational partition functions, EXC to account for ratios of populations above the ground vibrational level arising from the vibrational partition functions, and ZPE to account for the overall zero-point energy change for the reaction. The data shown in Table V compare the translational, rotational, MMI, and experimental values for the equilibrium constant of several of the isotopic replacement reactions examined here.

For the complete reaction in the hydronium ion, eq 37, the

$$H_3O^+(g) + \frac{3}{2}D_2O(g) \rightarrow D_3O^+(g) + \frac{3}{2}H_2O(g) \tag{37}$$

agreement between K_{MMI} and K_{expt} is seen to be excellent leading to the conclusion that either K_{EXC} and K_{ZPE} are both unity or that in this case they have a cancelling effect to give a $K_{EXC}{\cdot}K_{ZPE}$ product of near unity. An assessment of which of these is the more likely can be seen from a comparison of K_{MMI} and K_{expt} for the individual replacement reactions, eq 38–40. As the data in Table

$$H_3O^+(g) + \frac{1}{2}D_2O(g) \rightleftarrows H_2OD^+(g) + \frac{1}{2}H_2O(g) \tag{38}$$

$$H_2OD^+(g) + \frac{1}{2}D_2O(g) \rightleftarrows HOD_2^+(g) + \frac{1}{2}H_2O(g) \tag{39}$$

$$HOD_2^+(g) + \frac{1}{2}D_2O(g) \rightleftarrows D_3O^+(g) + \frac{1}{2}H_2O(g) \tag{40}$$

V reveal the MMI value for K_{38} is significantly greater than the experimental value, while the MMI value for K_{40} is significantly less than the experimental value. Good agreement between the MMI and experimental values for K_{39} is obtained however. A plausible explanation to rationalize each of these observations can be found in a consideration of the inversion mode, υ_2, of the hydronium ions. Ab initio calculations of the vibrational frequencies for H_3O^+[25,26] show that only υ_2 is of sufficiently low frequency to contribute to the EXC term. Similarly all modes of H_2O and D_2O are too high in frequency to contribute to a

Table VI.

species	geometry	moments of inertia (amu Å^2)
H_2O^a	r(O–H) = 0.958 Å (HOH) = 104.5°	I_A = 0.616 I_B = 1.155 I_C = 1.771
D_2O		I_A = 1.104 I_B = 2.313 I_C = 3.417
H_3O^+	r(O–H) = 0.975 Å (HOH) = 111.3°	I_A = 2.579 I_B = 1.571 I_C = 1.475
H_2OD^+		I_A = 3.365 I_B = 2.486 I_C = 1.524
HOD_2^+		I_A = 4.322 I_B = 2.464 I_C = 2.404
D_3O^+		I_A = 5.157 I_B = 3.080 I_C = 2.883
$H_5O_2^{+\,c}$	r(O–H$_t$) = 0.976 Å r(O–H$_b$) = 1.195 Å r(O–O) = 2.387 Å	I_A = 56.045 I_B = 54.954 I_C = 3.239
$D_5O_2^+$	(H$_t$OH$_b$) = 117.7° (H$_b$OH$_b$) = 109.4°	I_A = 66.999 I_B = 64.517 I_C = 6.176
$F(H_2O)^{-\,d}$	r(F–H$_b$) = 1.531 Å r(O–H$_b$) = 1.000 Å (F–H$_b$O) = 172° r(O–H$_t$) = 0.946 Å	I_A = 57.820 I_B = 0.826 I_C = 58.646
$F(D_2O)^-$		I_A = 60.136 I_B = 1.563 I_C = 61.699
$El(H_2O)^-$	r(Cl–H$_b$) = 2.415 Å r(O–H$_b$) = 0.961 Å (ClH$_b$O) = 154° r(O–H$_t$) = 0.947 Å	I_A = 126.489 I_B = 0.959 I_C = 127.448
$Cl(D_2O)^-$	(H$_t$OH$_t$) = 105.5°	I_A = 132.579 I_B = 1.869 I_C = 134.448

[a] Friedman, A. S.; Haar, L. *J. Chem. Phys.* **1954**, *22*, 2051. [b] Reference 28. [c] Reference 23. [d] Reference 24.

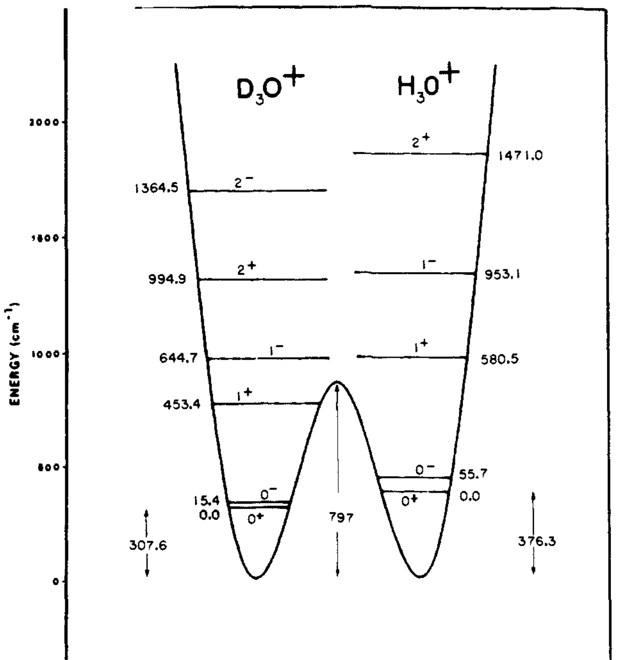

Figure 2. Potential function for the inversion mode (υ_2) of the hydronium ion including positions of the lowest few energy levels of H_3O^+ and D_3O^+ (taken from ref 28).

---

(23) Frisch, M. J.; Del Bene, J. E.; Binkley, J. S.; Schaeffer, H. F. *J. Chem. Phys.* **1986**, *84*, 2279.

(24) Gao, J.; Garner, D. S.; Jorgensen, W. L. *J. Am. Chem. Soc.* **1986**, *108*, 4784.

(25) DeFrees, D. J.; McLean, A. D. *J. Chem. Phys.* **1985**, *82*, 333.

(26) Colvin, M. E.; Raine, G. P.; Schaeffer, H. F.; Dupuis, M. *J. Chem. Phys.* **1983**, *79*, 1551.

(27) Melander, L.; Saunders, W. H. *Reaction Rates of Isotopic Molecules*; Wiley: New York, 1980.

(28) Sears, T. J.; Bunker, P. R.; Davies, P. B.; Johnson, S. A.; Spirco, V. *J. Chem. Phys.* **1985**, *83*, 2676.

deviation of K_{EXC} from 1.00. Fortunately the potential function for the inversion mode of both H_3O^+ and D_3O^+ have been well characterized by Sears et al.[28] The double minimum nature of the inversion potential gives rise to a splitting of each of the vibrational levels. In the case of H_3O^+ the inversion barrier is significantly lower than that in the isoelectronic NH_3, and hence the splitting is much greater. The inversion potential and the lowest energy levels for H_3O^+ and D_3O^+ are shown in Figure 2. In order to calculate an EXC term for such a set of levels the conventional harmonic oscillator form of the vibrational partition function cannot be used. Instead a direct summation must be used such that the K_{EXC} for eq 37 is given by eq 41, where the E_i are

$$K_{\mathrm{EXC}}(37) = \frac{\sum_i e^{-hcE_i/kT}(D_3O^+)}{\sum_i e^{-hcE_i/kT}(H_3O^+)} \qquad (41)$$

the energies in cm^{-1} of the *i*th level *above* the v_2 zero-point vibrational level of the species. By using the values in Figure 2, a value of K_{EXC} of 1.14 is obtained. The sum terms of 2.094 for D_3O^+ and 1.833 for H_3O^+ also reveal that a significant fraction of molecules populate levels other than the ground (0^+) state. Wolfsberg and Bron[29] have applied a similar analysis to isotopic replacement equilibria in NH_3 and ND_3 mixtures to assess the important of corrections to calculated equilibrium constants due to inversion. They concluded that for the ammonia system the correction would be less than 0.05%. However, in NH_3 the inversion barrier is much higher (2020 cm^{-1}), and the inversion splittings to the $v = 0$ level are very small (<1 cm^{-1}). Thus in that case the inversion mode is modelled well by a harmonic oscillator approximation. However, in the hydronium ion case the very low inversion barrier, the large inversion splittings, and the low lying 1^+, 1^-, and 2^+ states all contribute to a significant correction to the equilibrium constant due to inversion.

The value of K_{EXC} of 1.14 obtained for the complete replacement reaction, eq 37, implies that the zero-point energy contribution, K_{ZPE}, must be 0.9, that is, the products are of higher zero-point energy than reactants by approximately 36 cm^{-1}. It is noteworthy that the ratio of v_2 zero-point energies of H_3O^+ (376.3 cm^{-1}) and D_3O^+ (307.6 cm^{-1}) is significantly less than that for a typical harmonic oscillator system. Thus if this ratio was on the order of that expected for a normal harmonic system the zero-point energy change for the reaction would in fact have been negative rather than positive leading to a K_{ZPE} term greater than unity. This consideration may be used to explain the change in values of K_{38}–K_{40} relative to those calculated from the MMI terms. For each of these reactions, K_{EXC} can be anticipated to be greater than unity with each value increasing slightly with increasing deuterium content to give a product of 1.14. For the present argument values of 1.02, 1.04, and 1.07 will be assumed for the K_{EXC} portion of K_{38}, K_{39}, and K_{40}, respectively. These values require that the corresponding K_{ZPE} terms be 0.76, 0.95, and 1.17, respectively, consistent with overall zero-point energy changes of 57, 11, and −33 cm^{-1}. In other words with increasing deuterium substitution the zero-point energy changes become successively lower. This trend is exactly what is observed in the calculations of Schaeffer et al.[25] where harmonic frequencies for H_3O^+, H_2OD^+, HOD_2^+, and D_3O^+ were calculated and where the zero-point energy differences between each pair of species became increasingly negative with increasing deuterium substitution. Thus the experimentally observed equilibrium constants for eq 37–40 appear to be entirely consistent with statistical thermodynamic considerations.

Ab initio calculations indicate that the most stable form of $H_5O_2^+$ is a symmetrically hydrogen-bonded species of C_2 symmetry.[19] Frisch et al.[23] have calculated harmonic vibrational frequencies for such a species obtaining seven modes with frequencies below 800 cm^{-1}. For a system composed of a collection of harmonic oscillators whenever the mean vibrational frequency of the hydrogenic ion is less than that of H_2O the change in zero-point energy will be such as to favor accumulation of hydrogen in the ion rather than the neutral. In other words the zero-point energy term would make the calculated equilibrium constant *smaller*. However, the nature of the EXC term is such that species of lower vibrational frequencies favor accumulation of deuterium. The comparison of calculated and experimental equilibrium constants for $H_5O_2^+/D_5O_2^+$ indicates that the K_{EXC} term must dominate over the K_{ZPE} for a harmonic oscillator system. It is well known however that the hydrogen bond motions of $H_5O_2^+$ have a decidedly anharmonic potential. It would thus be highly desirable to have accurate anharmonic vibrational frequencies for both $H_5O_2^+$ and $D_5O_2^+$. The degree to which calculated ab initio frequencies can be used to reproduce the experimental isotope effect might then be taken as a measure of the accuracy of such calculations. In the absence of complete spectroscopic data for such ions these isotope effect experiments may then prove to be the best practical test of ab initio frequencies.

The relatively weak interaction of F^- with H_2O (23 kcal mol^{-1})[6] would indicate that the frequencies of the H_2O will be altered relatively little with three new low frequency modes introduced for motion of the hydrogen bond coordinate. Kistenmacher et al.[30] have obtained ab initio frequencies for a hypothetical C_{2v} $F(H_2O)^-$ complex. They justified doing calculations on such a species by noting that the potential was very flat between a C_{2v} form and the more stable nearly colinear hydrogen-bonded form. The frequencies obtained correspond to three values nearly equal to those of an isolated water molecule and three new frequencies of 292, 693, and 1238 cm^{-1} corresponding to motions of F^- relative to H_2O. Such a set of frequencies is not expected to lead to significant zero-point energy effects on the calculated equilibrium constant, and thus the difference between the experimental equilibrium constant of 0.66 and that obtained from K_{MMI} of 0.50 can be attributed primarily to the EXC terms. The vibrational contribution to the isotope effect will then arise principally from the low frequency hydrogen bond stretching modes.

The situation for Cl^-–H_2O is expected to be entirely analogous to that for $F(H_2O)^-$. In this case the interaction is even weaker, and H_2O frequencies will be even less perturbed leading to an even more negligible zero-point energy effect. However, since the hydrogen bond stretching motions will be of even lower frequency, the EXC terms will favor the $Cl(D_2O)^-$ complex even more over $Cl(H_2O)^-$. This is evident from the somewhat greater difference between the calculated and experimental isotope effects given in Table V.

The fact that gas-phase data for H_3O^+/D_3O^+ and data for these ions in acetonitrile solution[16] give virtually identical isotope effects indicate that the H_3O^+ ion in CH_3CN may be an isolated freely rotating entity. Thus H_3O^+–CH_3CN interactions introduce no significant perturbation of H_3O^+ motions in solution.

Similarly, consideration of the free energy changes in the gas phase for eq 42 and 43 of 0.25 and 0.16 kcal mol^{-1}, respectively,

$$F(H_2O)^- + D_2O \rightleftarrows F(D_2O)^- + H_2O \qquad (42)$$

$$Cl(H_2O)^- + D_2O \rightleftarrows Cl(D_2O)^- + H_2O \qquad (43)$$

show that fluoride transfer from H_2O to D_2O in the gas phase is $\approx$0.1 kcal mol^{-1} more endothermic than the corresponding chloride-transfer process.[31] In contrast solution phase data for these same reactions show that F^- transfer from H_2O to D_2O is approximately 0.1 kcal mol^{-1} more exothermic than the chloride transfer. Evidently in solution the greater ability of F^- to grow a larger solvation shell is associated with a more favorable environment for D_2O relative to H_2O than in the isolated F^- complexes of a single water molecule. One possibility is that the lower frequency modes associated with the more extensive hydrogen bonded network for F^- lead to a more favorable EXC contribution to the isotope effect. Swain and Bader[31] have specifically considered the model solution case of tetrahedrally coordinated water

---

(29) Bron, J.; Wolfsberg, M. *J. Chem. Phys.* **1972**, *57*, 2862.

(30) Kistenmacher, H.; Popkie, H.; Clements, E. *J. Chem. Phys.* **1973**, *59*, 5842.

(31) Swain, C. G.; Bader, R. F. W. *Tetrahedron* **1960**, *10*, 182.

molecules versus tetrahedrally coordinated monoatomic univalent ions and deduced that the nature of the solvent isotope effect is due to changes in librational frequencies of water induced by the presence of ions. Only F^- led to an increase in librational frequency with all other anions yielding decreases. These authors have thus interpreted the fluoride system as unique with solution in D_2O favored over H_2O because of the greater spacing of librational energy levels relative to pure water.

Conclusion

The equilibrium constants for isotope exchange reactions between gaseous water molecules and the four gaseous ions L_3O^+, $L_5O_2^+$, $(L_2O)F^-$, and $(L_2O)Cl^-$ have been determined from ion cyclotron resonance equilibrium techniques.

The value for isotopic fractionation factor of gaseous L_3O^+ is found to be essentially identical with that observed for isolated hydronium ion in acetonitrile. These result infers that hydrogen bonding from hydronium ion to acetonitrile in solution phase has a negligible effect on the fractionation factor. The results for L_3O^+ and $L_5O_2^+$ also fully support the results and conclusions drawn from experiments for these ions in aqueous solution. Specifically the increase in fractionation factor from gaseous hydronium ion to fully hydrated hydronium ion in solution is due to the extensive hydrogen bonding network present in solution. This is evident from the greater gas-phase fractionation factor of $L_5O_2^+$ relative to L_3O^+.

Hydrogen bonding of L_3O^+, F^-, and Cl^- to L_2O lowers the fractionation factors relative to that observed for gaseous H_2O. The effect of F^- on the fractionation factor is opposite to that expected on the basis of F^- behavior in aqueous solution and on the basis of relative F^- and Cl^- solution phase behavior. This is apparently associated with the dominance of zero-point energy effects on solution phase isotope effects, whereas in the gas phase for such small ions rotational contributions to the isotope effect become very important.

The experimental data consistently reveal that the mixed H/D species DOH_2^+, D_2OH^+, $H_3D_2O_2^+$, $(HOD)F^-$, and $(HOD)Cl^-$ are considerably less abundant than would be predicted on the basis of the "rule of the geometric mean" and the abundance of the fully deuteriated and protonated species. This is again almost certainly due to the combined importance of the MMI, EXC, and ZPE contributions to the overall isotope effects for such small ions.

The continued investigation of isotope effects for gaseous ions will hopefully provide further insights into the origin of such affects and lend credibility to mechanistic deductions based on isotope effects for solution phase ions. We would also suggest that the extent to which calculated vibrational frequencies used in statistical thermodynamic calculations of isotope effects are able to reproduce experimentally measured values will provide a rigorous measure of the level of the accuracy of vibrational frequencies. In particular temperature dependent studies are planned to obtain a measure of the ZPE component of some isotope effects.

Further, should spectroscopic investigations of the interstellar medium ultimately be successful in detecting H_3O^+, H_2OD^+, HOD_2^+, and D_3O^+ as a means of probing the existence of water the equilibra examined here will allow inference of the relative amounts of H_2O, HOD, and D_2O to be made.[32,33]

Acknowledgment. Financial support of this work by the National Sciences and Engineering Research Council of Canada (N.S.E.R.C.) and the Petroleum Research Fund of the American Chemical Society (ACS-PRF) is gratefully acknowledged. J. Fisher and C. Allison are thanked for assistance in calculations of moments of inertia.

Registry No. H^+, 12586-59-3; H_3O^+, 13968-08-6; F^-, 16984-48-8; Cl^-, 16887-00-6; D_2, 7782-39-0.

---

(32) Smith, D.; Adams, N. *Int. Rev. Phys. Chem.* **1981**, *1*, 271.
(33) Smith, D. *Philos Trans. Roy. Soc.* **1981**, *303*, 535.

Synchrotron Radiation Selected *s*-Tetrazine Ion Chemistry

I. Nenner,*[†] O. Dutuit,[‡] M. Richard-Viard,[§] P. Morin,[†] and A. H. Zewail[‖,⊥]

Contribution from LURE, Laboratoire mixte CNRS, CEA et MEN, Université de Paris Sud, Bât. 209 C, 91405 Orsay, Cedex, France.

Received June 19, 1987

Abstract: With use of synchrotron radiation (9–22 eV) the photon-selected chemistry of *s*-tetrazine ion is reported. Dissociation intermediates and products are investigated by the threshold photoelectron–photoion coincidence technique. On the basis of breakdown curves and thermodynamics, the loss of N_2 is found to be associated with the $C_2N_2H_2^+$ ion with an activation energy of 0.96 eV. Smaller fragment ions such as $HCNH^+$ and HCN^+ originate from single bond breaking of the $C_2N_2H_2^+$ primary fragment ion rather than the dissociation of the parent ion.

I. Introduction

The fragmentation of the *s*-tetrazine molecule ($C_2N_4H_2$) into one N_2 and two HCN molecules[1,2] after its photoexcitation to the lowest singlet states has raised several questions.[3,4] One question concerns the identification of the "active" excited state which can be reached with a single photon in the visible or near-UV spectrum. Another deals with the dynamics of the photodissociation process itself, which involves either a direct triple fragmentation through a specific transition state or a sequential dissociation.[3-5] The consensus appears to be in favor of a simultaneous triple fragmentation.[3-5] However, it is difficult to prove such a mechanism.

In this paper we report studies of the fragmentation of *s*-tetrazine ion, photoselected by synchrotron radiation in the energy

---

[†] CEA-IRDI/DESICP-Département de Physico-Chimie, 91191 Gif sur Yvette, Cedex, France.

[‡] LPCR, U.A. 75, Université Paris Sud, Bât. 350, 91405 Orsay, Cedex, France.

[§] LCAM, U.A. 281, Université Paris Sud, Bât. 351, 91405 Orsay, Cedex, France.

[‖] A. A. Noyes Laboratory of Chemical Physics, California Institute of Technology, Pasadena, CA 91125. Contribution No. 7606.

[⊥] John Simon Guggenheim Foundation Fellow.

(1) Hochstrasser, R. M.; King, D. S. *J. Am. Chem. Soc.* **1975**, *97*, 4760.
(2) Coulder, D.; Dows, D.; Reisler, H.; Wittig, C. *Chem. Phys.* **1978**, *32*, 429.
(3) King, D. S.; Denny, C. T.; Hochstrasser, R. M.; Smith, A. B. *J. Am. Chem. Soc.* **1977**, *99*, 271.
(4) Glownia, J. H.; Riley, S. J. *Chem. Phys. Lett.* **1980**, *71*, 429.
(5) Scheiner, A. C.; Scuseria, G. E.; Schaeffer, H. F., III *J. Am. Chem. Soc.* **1986**, *108*, 8160.

0002-7863/88/1510-1093$01.50/0